Acta Crystallographica Section B
Structural Science
ISSN 0108-7681

Dopant positions in strontium/chromium- and barium-doped KTP, determined with synchrotron X-radiation

Stefan T. Norberg,[a]* Victor A. Streltsov,[b] Göran Svensson[a] and Jörgen Albertsson[a]

[a]Inorganic Chemistry, Chalmers University of Technology, SE-412 96 Göteborg, Sweden, and [b]Crystallography Centre, University of Western Australia, Nedlands 6907, Australia

Correspondence e-mail: stn@inoc.chalmers.se

Received 22 May 2000
Accepted 19 September 2000

Structure factors for strontium/chromium- (Sr/Cr) and barium- (Ba) doped potassium titanyl phosphate ($KTiOPO_4$, KTP) were measured with focused synchrotron X-radiation [0.75000 (9) Å] using a fast avalanche photodiode counter. Space group $Pna2_1$, $Z = 8$, $a = 12.786$ (2), $b = 6.3927$ (8), $c = 10.5585$ (9) Å, $T = 293$ (1) K, $R = 0.028$ (SrCrKTP); $a = 12.851$ (6), $b = 6.418$ (3), $c = 10.620$ (5) Å, $T = 120$ (1) K, $R = 0.031$ (BaKTP). The refinement of the dopant positions showed that Ba^{2+} is positioned in the larger of the two K cavities of KTP, while the smaller Sr^{2+} ion is located in both. Split positions are found for the strontium dopant in both cavities and they are located in the positive c direction from the potassium cation. The chromium dopant has two different oxidation states, namely +III and +VI; in both states the dopant is located inside the TiO_6 octahedra. The two structures show slightly less distorted TiO_6 octahedra than pure KTP.

1. Introduction

Since the structural determination of $KTiOPO_4$ (KTP, potassium titanyl phosphate) by Tordjman *et al.* (1974), KTP has evolved to a well known material for nonlinear optical applications. The high nonlinearity and optical damage threshold extend to many isomorphic compounds with the general chemical formula $MTiOXO_4$ (most common are M = K, Rb, Cs or Tl and X = P or As). Much effort has been spent studying the effect of different monovalent cation dopants and other isomorphic substitutions with respect to optical parameters, crystal growth properties and structural effects (Stucky *et al.*, 1989, and references therein). So far, KTP crystals doped with divalent cations have attracted less interest. Chu *et al.* (1993) and Roelofs *et al.* (1991) described changes in the crystal properties due to doping of KTP with strontium and barium, although none of these studies were based on flux-grown crystals. Instead, the dopants were introduced into the KTP crystals by ion exchange in nitrate melts. Changes in the Curie temperature and ferroelectric/dielectric behaviour for barium-doped KTP were measured by Chu *et al.* (1993). Barium-doped KTP exhibits a decrease in Curie temperature when the barium concentration is increased, *e.g.* 1.27% barium results in a Curie temperature which is 50 K lower than that for pure KTP. The pure KTP has a T_c value of 1207 K (Stefanovich *et al.*, 1996).

Other reasons to study KTP doped with strontium and barium cations are that barium is used to make periodically poled waveguides in KTP crystals and that $KBa_2(PO_3)_5{\cdot}2K_2O$ was proposed by Suma *et al.* (1998) as a new flux for fast

growth. The use of this flux gave large crystals during a 1 d growth period. It was also noted that a small amount of barium had been incorporated in the crystals.

One way of creating periodically polarized domains is by electric field poling. Risk & Lau (1996) reported good results with KTP crystals subjected to ion exchange in an $RbNO_3$/$Ba(NO_3)_2$ melt. They introduced the ion exchange selectively in some areas of the crystal. These areas had different electric field poling properties owing to the addition of barium and rubidium in the surface layer. By applying an electric field over the crystal in the polar direction, waveguides can be made. Areas, which have been subjected to ion exchange, do not change polarity owing to high ionic conductivity. Conductivity in KTP takes place by diffusion of the potassium ions *via* a vacancy mechanism (Furusawa *et al.*, 1993), and ionic diffusion in KTP is enhanced by the addition of divalent cations which introduce extra vacancies in the cation sublattice. Knowledge on positions of divalent cations in the KTP structures should help in understanding the properties of the KTP-type materials.

Another method developed by Karlsson & Laurell (1997) for producing quasi-phase matched nonlinear frequency conversion with KTP utilizes the fact that a pure $RbNO_3$ melt decreases the ionic conductivity. Obviously, the vacancies created by the addition of barium influence the results of a poling experiment. Daneshvar *et al.* (1997) reported that the addition of as little as 0.1% barium to a $RbNO_3$ melt significantly increases the ion exchange depth of rubidium in KTP.

Recently, attention has been drawn to cation split positions in KTP, although there are few examples of structural refinement of these small shifts in position. Different cation positions are in most cases just a result of the mixture of different cations in the crystal structure. However, cation split positions have also been found in pure nondoped KTP isomorphic structures and in mixed cation materials of the KTP family. Belokoneva *et al.* (1990) observed cation split positions for potassium in the KTP-like material $KFeFPO_4$ and they mentioned the existence of a similar phenomenon in KTP. Using high-resolution X-ray diffraction experiments for KTP, Delarue *et al.* (1999) found that the potassium cations do split at two or more positions at higher temperatures (673 K and above). Similar split position phenomena were for example found in pure $CsTiOAsO_4$ (Nordborg, 2000), pure $RbTiOAsO_4$ (Streltsov *et al.*, 2000) and $Cs_xRb_{1-x}TiOAsO_4$ (Thomas & Womersley, 1998). The structural effects of strontium and barium in KTP have not been studied before, which suggests an investigation of the possibility of split positions in the divalent doped KTP crystals.

We report here the structures of KTP crystals containing strontium and chromium (SrCrKTP) and barium (BaKTP), respectively. Diffraction data have been collected with synchrotron X-rays at the Photon Factory in Tsukuba, Japan. It should be noted that the barium-doped KTP also incorporated a minuscule amount of Cr^{3+}, which could not be detected in the X-ray diffraction experiments.

2. Experimental

2.1. Preparation of crystals

Crystals of SrCrKTP and BaKTP were obtained by spontaneous flux crystallization in platinum crucibles. An attempt to increase the level of the divalent doping was made by adding some amount of Cr^{3+} to the flux, which could facilitate a double exchange of cations resulting in the formation of $K_xM_{1-x}Ti_yCr_{1-y}PO_4$ (M^{2+} rather than K^+ and simultaneously Cr^{3+} rather than Ti^{4+}). For the SrCrKTP crystallization a mixture of $SrCO_3$, Cr_2O_3, TiO_2, KH_2PO_4 and K_2HPO_4 with a molar ratio of 1.96:1:3.96:17.1:7.22 was used. This resulted in a flux with a K^+/Sr^{2+} ratio of 16.1:1 and a Ti^{4+}/Cr^{3+} ratio of 1.98:1. BaKTP was crystallized using a mixture of $Ba(NO_3)_2$, Cr_2O_3, TiO_2, KH_2PO_4 and K_2HPO_4 with a molar ratio of 10.3:1:18.7:64.9:8.3, thus giving a K^+/Ba^{2+} ratio of 7.9:1 and Ti^{4+}/Cr^{3+} ratio of 9.4:1. Both mixtures were slowly heated for 4 d in order to obtain a homogeneous melt. The SrKTP melt was heated to 1373 K, then the temperature was decreased to 1093 K by 1.2 K h^{-1}. The BaKTP melt was heated to 1273 K and then cooled to 1023 K by 1.4 K h^{-1}. The resulting crystals were easily recovered by dissolving the flux in water. The SrCrKTP batch was a mixture of different crystals, which were predominantly large green crystals of $KTi_2(PO_4)_3$ (Masse *et al.*, 1972) doped with chromium. The KTP crystals containing strontium and chromium had a light brown color, indicating the presence of Cr^{VI}. The BaKTP batch was composed of crystals with the typical KTP morphology (Bolt & Bennema, 1990). These crystals had a light green–brown color, indicating some Cr inclusion.

2.2. Data collection

Small as-grown crystals were used for the data collection at the Photon Factory, Tsukuba, using the beamline 14A four-circle diffractometer (Satow & Iitaka, 1989). Details of the measurements are given in Table 1.[1] Vertically polarized X-radiation (polarization ratio ~0.95) from a vertical wiggler was monochromated by a double Si(111) perfect crystal monochromator, and focused using a curved fused quartz mirror coated with Pt. The beam optics were automatically adjusted every 20 min for maximum flux. A high-speed avalanche photodiode (APD) detector with a counting linearity up to 10^8 c.p.s. was used (Kishimoto *et al.*, 1998). The experimental set-up was similar to that described by Streltsov *et al.* (1998).

SrCrKTP was measured at room temperature and BaKTP at 120 K using synchrotron X-radiation with $\lambda = 0.75000$ (9) Å. The measured intensities were normalized using the incident beam intensities monitored during each scan. The intensity decay was carefully monitored during each experiment with six standard reflections. The intensity of the standard reflections during the SrCrKTP experiment was relatively stable until the latter parts of each storage ring injection periods,

[1] Supplementary data for this paper are available from the IUCr electronic archives (Reference: OS0060). Services for accessing these data are described at the back of the journal.

Table 1
Experimental details.

Computer programs: BL14A (Tsukuba, Japan); *Xtal*3.6 (Hall *et al.*, 1999) *DIFDAT, ADDREF, ABSORB, SORTRF*, *CRYLSQ*, *BONDLA, ATABLE, CIFIO*.

	SrCrKTP	BaKTP
Crystal data		
Chemical formula	$Sr_{0.06}K_{0.87}Cr_{0.05}Ti_{0.95}OPO_4$	$Ba_{0.06}K_{0.88}TiOPO_4$
Chemical formula weight	198.13	201.6
Cell setting, space group	Orthorhombic, $Pna2_1$	Orthorhombic, $Pna2_1$
a, b, c (Å)	12.786 (2), 6.3927 (8), 10.5585 (9)	12.851 (6), 6.418 (3), 10.620 (5)
V (Å^3)	863.03 (19)	876.0 (7)
Z	8	8
D_x (Mg m^{-3})	3.050	3.057
Radiation type	Synchrotron X-ray	Synchrotron X-ray
Wavelength (Å)	0.75000	0.75000
No. of reflections for cell parameters	12	12
θ range (°)	35.9–44.8	25.3–45.0
μ (mm^{-1})	4.107	3.605
Temperature (K)	293 (1)	120 (1)
Crystal form, color	Rectangular, light brown	Prism, light green–brown
Crystal size (mm)	0.058 × 0.054 × 0.040	0.032 × 0.024 × 0.016
Data collection		
Diffractometer	BL14*A* four-circle	BL14*A* four-circle
Data collection method	ω–2θ scans	ω–2θ scans
Absorption correction	Analytical	Analytical
T_{min}	0.8054	0.8959
T_{max}	0.8577	0.9446
No. of measured, independent and observed reflections	40 331, 10 124, 10 124	10 098, 2663, 2631
Criterion for observed reflections	$F > 2\sigma(F)$	$F > 2\sigma(F)$
R_{int}	0.060	0.079
θ_{max} (°)	64.91	32.38
Range of h, k, l	$-28 \rightarrow h \rightarrow 28$ $-14 \rightarrow k \rightarrow 14$ $-25 \rightarrow l \rightarrow 23$	$-18 \rightarrow h \rightarrow 18$ $-9 \rightarrow k \rightarrow 9$ $-15 \rightarrow l \rightarrow 15$
No. of standard reflections and frequency	6, every 200 reflections	6, every 94 reflections
Intensity decay (%)	23	2
Refinement		
Refinement on	F	F
R, wR, S	0.028, 0.032, 2.493	0.031, 0.045, 2.97
No. of reflections/parameters used in refinement	10 124/194	2631/150
H-atom treatment	None	None
Weighting scheme	$w = 1/\sigma^2(F)$	$w = 1/\sigma^2(F)$
$(\Delta/\sigma)_{max}$	0.019	0.001
$\Delta\rho_{max}, \Delta\rho_{min}$ (e Å^{-3})	1.199, −1.454	0.722, −0.721
Extinction method	Gaussian (Zachariasen, 1967)	Gaussian (Zachariasen, 1967)
Extinction coefficient	–	9 (3) × 10^3

where it dropped by approximately 23% each time. A correction for this decay was made. The range of used reflections in the refinement of BaKTP was reduced to a maximum resolution of $\theta = 32.4°$, owing to significant fluctuation (∼2%) of the recorded standard reflections giving an larger impact on the weaker high θ reflections. An ω scan width of 0.55° was used for both data collections. Reflection intensities were measured using ω–2θ continuous time scans with a sampling time of 10 ms per step.

2.3. Structure refinement

Details of the refinements can be found in Table 1. Anomalous scattering factors for neutral atoms for the appropriate wavelength were taken from Sasaki (1989). Symmetrically equivalent reflections were averaged, while keeping the Friedel mates separated. All integrated intensities were subjected to a Fisher test (Hamilton, 1964); intensities consistent with the measurement statistics were retained and the others were adjusted according to the scattering of equivalents. The linear absorption coefficient μ was calculated using mass attenuation coefficients for neutral atoms at wavelength 0.75 Å (Sasaki, 1990). An analytical absorption correction (Alcock, 1974) was applied for both crystals. All computations were made with the *Xtal*3.6 package (Hall *et al.*, 1999).

SrCrKTP was first refined as KTP without dopants and coordinates were taken from Almgren *et al.* (1999). The resulting structural model refined to $R = 0.041$, $wR = 0.052$, $S = 4.04$ and to the residual electron density $\Delta\rho_{max}/\Delta\rho_{min}$ of 4.84/−1.63 e Å^{-3}. Three peaks with a significantly high positive $\Delta\rho$ were found in the vicinity of the K1 and K2 sites and one peak inside each TiO_6 octahedra. From the resulting $\Delta\rho$ maps (Fig. 1) possible positions for the Sr and Cr dopants were located. Three Sr locations including two sites at ∼0.5 and ∼1.4 Å from K1 and one at ∼0.5 Å from K2 in the positive c direction were refined. Possible sites for the chromium dopant were located inside each TiO_6 octahedra close (0.40 Å) to the Ti atoms. The initial occupation parameters for the additional atoms were set to 0.1. The sum of the total occupancies inside each TiO_6 octahedra was fixed to 1.0. This model converged to $R = 0.030$, $wR = 0.036$, $S = 2.78$ with a $\Delta\rho_{max}/\Delta\rho_{min}$ of 2.07/−1.41 e Å^{-3}. One new significant positive peak was found at ∼1.4 Å from K2 in the positive c direction. The strontium positions are refined as Sr1*a*, Sr1*b*, Sr2*a* and Sr2*b* with the first two in the vicinity of K1 (Sr1*a* is closer to K1) and a similar arrangement for Sr2*a* and Sr2*b* in the vicinity of K2. The final cycles of refinement using only the constraint mentioned above resulted in the $\Delta\rho$ maps without significantly high peaks of positive residual electron density and $R = 0.028$, $wR = 0.032$, $S = 2.49$ and $\Delta\rho_{max}/\Delta\rho_{min}$ of 1.20/−1.45 e Å^{-3}. Anisotropic displacement parameters were refined for all atoms except Cr2.

An isotropic extinction parameter (Zachariasen, 1967) was refined using Larson's implementation (Larson, 1970). No extinction was found for this crystal. The Flack (1983) parameter was refined to 0.46 (1), which suggests that the crystal is nearly an equal mixture of domains of opposite polarization. The atomic fractional coordinates, occupation and displacement parameters for $Sr_{0.06}K_{0.87}Cr_{0.05}Ti_{0.95}OPO_4$ are listed in Table 2.

Initial refinement of BaKTP were carried out as described above for SrCrKTP with the result $R = 0.040$, $wR = 0.059$, $S = 3.85$ and $\Delta\rho_{max}/\Delta\rho_{min}$ of 1.54/−0.85 e Å^{-3}. It was found that one peak of high positive residual electron density was situated at the K2 site. This excess residual density was attributed to a contribution from barium at the K2 site. The barium cation is slightly larger than the potassium cation in this material, as indicated by the larger unit cell compared with that for pure KTP. Hence, barium should preferably be located in the larger K2 cavity. Replacing K2 completely with barium resulted in a very poor R value and extremely large atomic displacement parameters (U^{ij}). Refinement with a mixture of barium and potassium at the K2 site improved the structural model, especially the displacement parameters for most atoms. For instance, the large differences between K1 and K2 [U_{eq} = 0.0098 (7) Å^2 for K1 and 0.0033 (5) Å^2 for K2] disappeared after the addition of barium in the K2 position [new U_{eq} = 0.0081 (6) Å^2 for K1 and 0.007 (2) Å^2 for K2]. An initial population of 0.1 was chosen for Ba2 and no constraints were used for the population of K1, K2 and Ba2. Refinement of K2 and Ba2 separately allowing for split cation sites resulted in the same refinement indices as for a model with the same mixed K2/Ba2 position: $R = 0.031$, $wR = 0.045$, $S = 2.97$ and a $\Delta\rho_{max}/\Delta\rho_{min}$ of 0.72/−0.72 e Å^{-3}. In this case all structural parameters change within 1 s.u., except for the K2 and Ba2 positions which were separated by 0.14 (3) Å, which is too small to be physically meaningful. All atomic displacements except Ba2 were treated anisotropically.

An isotropic extinction parameter was refined as for SrCrKTP. About 4% of the reflections were affected by extinction with a maximum correction of $y = 0.95$ for the 00±4 reflections. The observed structure factor is $F_{obs} = yF_{kin}$, where F_{kin} is the kinematic value of the structure factor. The refined Flack parameter of 0.56 (5) again suggests that this crystal is also a mixture of domains with opposite polarization. Table 3 gives atomic fractional coordinates, and occupation and displacement parameters for the $Ba_{0.06}K_{0.88}TiOPO_4$ structure.

Table 2
Fractional atomic coordinates and equivalent isotropic displacement parameters (Å^2).

$$U_{eq} = (1/3)\Sigma_i\Sigma_j U^{ij}a^i a^j \mathbf{a}_i.\mathbf{a}_j.$$

	x	y	z	U_{eq}	Occupancy
K1	0.37755 (5)	0.22053 (9)	0.30331 (8)	0.01901 (18)	0.857 (2)
Sr1*a*	0.3898 (6)	0.2116 (9)	0.3398 (8)	0.019 (2)	0.040 (1)
Sr1*b*	0.3945 (9)	0.2022 (17)	0.4372 (12)	0.026 (4)	0.023 (1)
K2	0.10548 (4)	0.30046 (11)	0.05796 (8)	0.0204 (2)	0.882 (2)
Sr2*a*	0.1047 (6)	0.3032 (11)	0.0968 (8)	0.016 (2)	0.033 (1)
Sr2*b*	0.1219 (10)	0.2783 (13)	0.1953 (11)	0.025 (4)	0.020 (1)
Ti1	0.372899 (17)	0.49998 (3)	−0.00666 (6)	0.00705 (6)	0.955 (1)
Cr1	0.3874 (5)	0.5069 (7)	0.0214 (6)	0.0096 (7)	0.045 (1)
Ti2	0.246829 (14)	0.73301 (4)	0.24415 (7)	0.00664 (6)	0.948 (1)
Cr2	0.2450 (3)	0.7862 (6)	0.2666 (5)	0.0096 (13)	0.052 (1)
P1	0.498123 (18)	0.66508 (4)	0.25210 (9)	0.00661 (7)	
P2	0.18034 (2)	0.49796 (4)	0.50376 (6)	0.00665 (9)	
O1	0.48594 (9)	0.51487 (18)	0.14126 (12)	0.0111 (3)	
O2	0.50963 (8)	0.5347 (2)	0.37442 (11)	0.0110 (3)	
O3	0.40048 (6)	0.80241 (15)	0.27093 (10)	0.0098 (3)	
O4	0.59383 (6)	0.80702 (15)	0.23196 (10)	0.0101 (3)	
O11	0.27536 (8)	0.53370 (16)	0.13381 (11)	0.0105 (3)	
O12	0.22366 (8)	0.9591 (2)	0.38055 (12)	0.0113 (3)	
O5	0.11202 (9)	0.68890 (17)	0.53274 (11)	0.0097 (3)	
O6	0.11110 (9)	0.30816 (16)	0.47780 (11)	0.0109 (3)	
O7	0.25287 (8)	0.4608 (2)	0.61869 (12)	0.0111 (3)	
O8	0.25264 (8)	0.53903 (18)	0.390 (2)	0.0111 (3)	

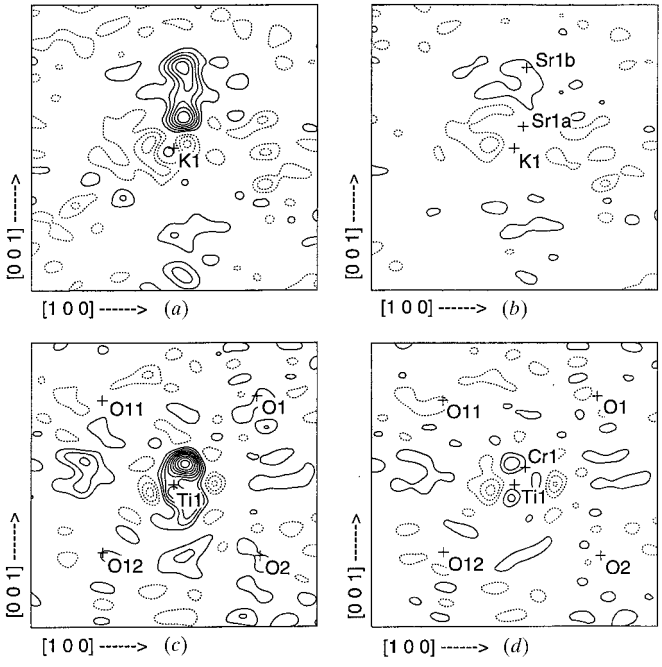

Figure 1
$\Delta\rho$ maps in the (010) plane for SrCrKTP drawn with positive and negative contours as solid lines and dashed lines, respectively, at increments of 0.4 e Å^{-3} [$\sigma(\Delta\rho)$ = 0.17 e Å^{-3}]. The zero contour is omitted. The maps show $\Delta\rho$ (*a*) before and (*b*) after the addition of strontium near the K1 positions and $\Delta\rho$ (*c*) before and (*d*) after the addition of chromium near the Ti1 position. Sr1*a* is 0.05 and Sr1*b* is 0.11 Å above the plane in (*b*), whereas in (*d*) Cr1 is 0.04 Å below the plane. All oxygens in (*c*) and (*d*) are within ± 0.3 Å of the plane. Map borders are 5 × 5 Å.

3. Result and discussion

Both $Sr_{0.06}K_{0.87}Cr_{0.05}Ti_{0.95}OPO_4$ and $Ba_{0.06}K_{0.88}TiOPO_4$ have the normal KTP structure (Tordjman *et al.*, 1974) of strongly distorted TiO_6 octahedra with corners linked alternatively *cis* and *trans* to form helical chains in the [011] direction through the crystal structure. They are further bridged by PO_4 tetrahedra and form TiO_6—PO_4—TiO_6 chains giving an open framework with large cavities for the cations to occupy. Fig. 2(*a*) shows how the strontium split positions in SrCrKTP are

placed in the TiO_6—PO_4 framework. Sr1*a*, Sr1*b*, Sr2*a* and Sr2*b* are shifted in the positive *c* direction from K1 and K2, respectively. The distances between the different cation sites are as follows: K1—Sr1*a* 0.419 (8), K1—Sr1*b* 1.43 (1), K2—Sr2*a* 0.409 (9) and K2—Sr2*b* 1.47 (1) Å. The strontium dopant is regularly placed in the KTP framework with a slight preference for the K1 cavity, while the barium position (Fig. 2*b*) in the BaKTP crystal is in the larger K2 cavity. This preference of a specific site has been previously reported for other mixed KTP isomorphs. Some examples are $Na_xK_{1-x}TiOPO_4$ (Crennell *et al.*, 1992), $Rb_xK_{1-x}TiOPO_4$ (Crennell *et al.*, 1991; Thomas *et al.*, 1994) and $Cs_xRb_{1-x}TiOAsO_4$ (Womersley *et al.*, 1998). The phenomenon is often more pronounced when the overall dopant concentration is low.

There are no large differences between the doped KTP crystals described here and the non-doped KTP crystal refined by Thomas *et al.* (1990), regarding the distortion of the TiO_6 octahedra. The s.u. from the mean bond distances are somewhat smaller in all the TiO_6 octahedra of the doped crystals than in pure KTP, as shown in Table 4. There is a significant but small decrease in the max/min bond distances in both TiO_6 octahedra of SrCrKTP and BaKTP. An investigation by Almgren *et al.* (1999) on the $RbTiOAsO_4$ structure at 9.6 K and room temperature shows that the changes of the standard deviations due to the temperature are small (less than 0.003 Å), so the differences between BaKTP (120 K) and KTP (room temperature) are not an artefact of the different temperatures. This means that the TiO_6 octahedra are more ordered and closer to the *Pnan* symmetry, which is the symmetry of the paraelectric high-temperature phase of KTP first reported by Thomas *et al.* (1990).

Table 3
Fractional atomic coordinates and equivalent isotropic displacement parameters (Å^2).

$$U_{eq} = (1/3)\Sigma_i\Sigma_j U^{ij} a^i a^j \mathbf{a}_i.\mathbf{a}_j.$$

	x	*y*	*z*	U_{eq}	Occupancy
K1	0.37678 (11)	0.2210 (2)	0.30754 (18)	0.0081 (6)	1.000 (4)
K2	0.1073 (11)	0.300 (2)	0.0568 (13)	0.007 (2)	0.755 (10)
Ba2	0.104 (2)	0.305 (4)	0.069 (2)	0.006 (3)	0.123 (3)
Ti1	0.37269 (8)	0.50034 (16)	0.00013 (17)	0.0038 (4)	
Ti2	0.24644 (9)	0.73294 (16)	0.25070 (16)	0.0035 (4)	
P1	0.49818 (13)	0.6639 (2)	0.2582 (2)	0.0030 (6)	
P2	0.18075 (11)	0.4977 (2)	0.5104 (2)	0.0032 (6)	
O1	0.4863 (4)	0.5128 (7)	0.1485 (4)	0.006 (2)	
O2	0.5098 (4)	0.5347 (8)	0.3815 (4)	0.005 (2)	
O3	0.4003 (4)	0.8019 (7)	0.2769 (4)	0.006 (2)	
O4	0.5937 (3)	0.8077 (7)	0.2389 (4)	0.0044 (19)	
O11	0.2752 (4)	0.5333 (7)	0.1403 (4)	0.005 (2)	
O12	0.2238 (4)	0.9586 (8)	0.3873 (4)	0.005 (2)	
O5	0.1118 (4)	0.6887 (7)	0.5385 (4)	0.005 (2)	
O6	0.1110 (4)	0.3085 (7)	0.4852 (4)	0.006 (2)	
O7	0.2530 (4)	0.4608 (8)	0.6259 (4)	0.006 (2)	
O8	0.2530 (4)	0.5388 (8)	0.397 (3)	0.005 (2)	

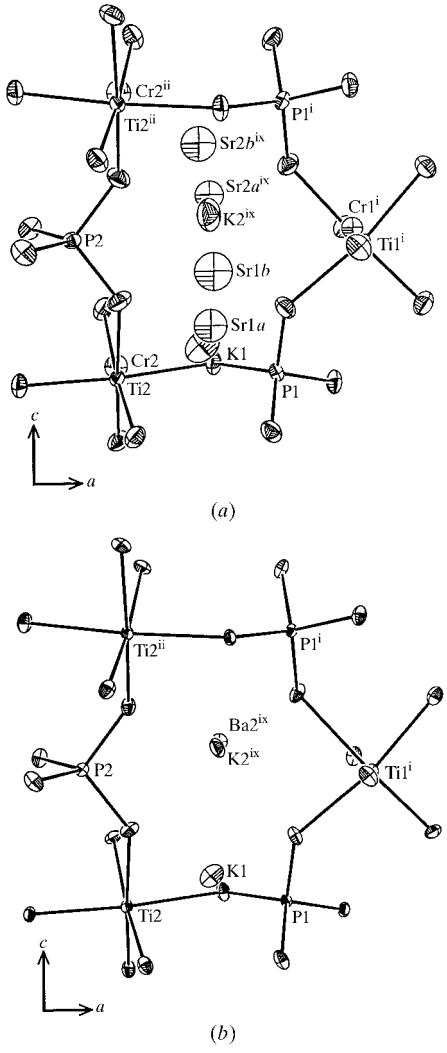

Figure 2
*ORTEP*III (Burnett & Johnson, 1996) views in the (010) plane of the structure of (*a*) SrCrKTP and (*b*) BaKTP. Displacement ellipsoids for both structures are drawn at the 80% probability level. Symmetry codes are given in Table 5.

Table 5 compares the cation–oxygen distances for KTP (Thomas *et al.*, 1990), SrCrKTP and BaKTP, whereas Fig. 3 shows the coordination around the K and Sr positions in the K2 cavity of SrCrKTP. The coordination for the two strontium positions in each cavity differs significantly from that of the K atom. In order to compare the different coordination environments in the two structures only the cation—oxygen bond lengths below 3.06 Å are included for strontium and potassium. The average bond distance for K1 and K2 to the surrounding O atoms is very similar in KTP, SrCrKTP and BaKTP, while Sr1*a*, Sr1*b*, Sr2*a* and Sr2*b* have substantially shorter mean bond distances to the coordinating O atoms. The smaller strontium ion does not fit so well as potassium in the larger K2 cavity, as indicated by the s.u. of the mean bond distance, which is significantly higher for Sr2*a* and Sr2*b* than for Sr1*a* and Sr1*b*.

The brown color of the SrCrKTP crystal and the Cr—O bond lengths listed in Table 6 clearly indicate the existence of Cr atoms with different oxidation states. Cr1 is located near the centroid of the distorted $Ti1O_6$ octahedron with a shortest Cr1—O bond of 1.782 (7) Å. Cr2 is in a different environment

Table 4
Bond lengths (Å) for the TiO_6 octahedra in KTP, SrCrKTP and BaKTP.

	KTP	SrCrKTP	BaKTP
Ti1—O2^{i}	1.958 (3)	1.9702 (12)	1.979 (5)
Ti1—O11	1.981 (2)	1.9498 (12)	1.957 (5)
Ti1—O12^{ii}	1.716 (2)	1.7352 (13)	1.745 (5)
Ti1—O5^{ii}	2.042 (3)	2.0408 (11)	2.051 (5)
Ti1—O6^{iii}	1.987 (3)	1.9875 (11)	1.995 (5)
Mean Ti1—O	1.97 (14)	1.97 (13)	1.98 (13)
Ti2—O3	2.044 (3)	2.0339 (9)	2.045 (5)
Ti2—O4^{iv}	1.981 (3)	1.9771 (9)	1.984 (5)
Ti2—O11	1.733 (3)	1.7646 (12)	1.776 (5)
Ti2—O12	2.092 (4)	2.0618 (14)	2.071 (5)
Ti2—O7^{iii}	1.965 (4)	1.9686 (14)	1.973 (5)
Ti2—O8	1.990 (3)	1.981 (18)	1.99 (2)
Mean Ti2—O	1.97 (12)	1.96 (10)	1.97 (10)

The s.u. of the mean is calculated as: $[\Sigma(x-\bar{x})^2/n-1]^{1/2}$. Symmetry codes: (i) $1-x, 1-y, z-\frac{1}{2}$; (ii) $\frac{1}{2}-x, y-\frac{1}{2}, z-\frac{1}{2}$; (iii) $\frac{1}{2}-x, \frac{1}{2}+y, z-\frac{1}{2}$; (iv) $x-\frac{1}{2}, \frac{3}{2}-y, z$.

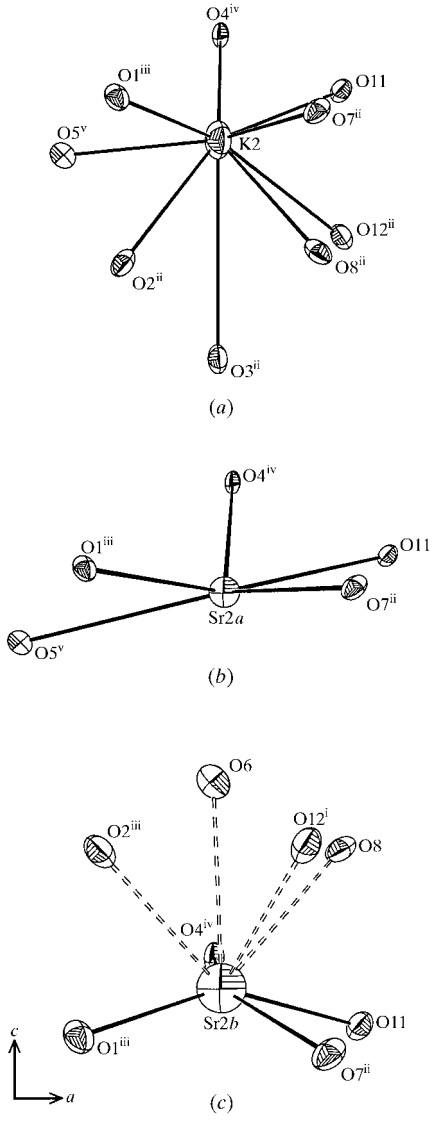

Figure 3
*ORTEP*III (Burnett & Johnson, 1996) views of the coordination around the cations in the larger K2 cavity in the (010) plane of SrCrKTP. Displacement ellipsoids and symmetry codes as in Table 5.

Table 5
The K—O, Sr—O and Ba—O bond lengths (Å) in KTP, SrCrKTP and BaKTP.

For BaKTP: note that the mean bond and s.u. are based on bond lengths < 3.06 Å for K and Sr.

KTP (*a*)		SrCrKTP	
K1—O1	2.894 (3)	K1—O1	2.8963 (14)
K1—O2	2.738 (3)	K1—O2	2.7294 (13)
K1—O3^{i}	2.712 (3)	K1—O3^{i}	2.7106 (12)
K1—O11	2.996 (3)	K1—O11	2.9863 (13)
K1—O12^{i}	2.722 (3)	K1—O12^{i}	2.7073 (13)
K1—O5^{ii}	2.872 (2)	K1—O5^{ii}	2.8671 (14)
K1—O7^{ii}	3.057 (3)	K1—O7^{ii}	3.0557 (14)
K1—O8	2.755 (3)	K1—O8	2.746 (8)
Mean K1—O	2.84 (13)	Mean K1—O	2.84 (13)
K2—O1^{iii}	2.677 (3)	Sr1*a*—O1	3.109 (7)
K2—O2^{ii}	2.982 (3)	Sr1*a*—O2	2.598 (6)
K2—O3^{ii}	3.045 (2)	Sr1*a*—O3^{i}	2.718 (6)
K2—O4^{iv}	3.117 (3)	Sr1*a*—O12^{i}	2.702 (7)
K2—O11	2.765 (3)	Sr1*a*—O6^{vi}	3.185 (7)
K2—O12^{ii}	3.057 (3)	Sr1*a*—O8	2.782 (8)
K2—O5^{v}	2.806 (3)	Mean Sr1*a*—O	2.70 (7)
K2—O7^{ii}	2.918 (3)		
K2—O8^{ii}	3.048 (3)	Sr1*b*—O1^{vii}	3.202 (12)
Mean K2—O	2.91 (15)	Sr1*b*—O2	2.669 (11)
		Sr1*b*—O3^{i}	3.102 (11)
BaKTP		Sr1*b*—O4^{vii}	3.116 (13)
K1—O1	2.888 (5)	Sr1*b*—O11^{viii}	3.192 (12)
K1—O2	2.756 (5)	Sr1*b*—O12^{i}	2.747 (11)
K1—O3^{i}	2.726 (5)	Sr1*b*—O6^{vi}	2.803 (11)
K1—O11	2.979 (5)	Sr1*b*—O7	3.112 (12)
K1—O12^{i}	2.724 (5)	Sr1*b*—O8	2.858 (12)
K1—O5^{ii}	2.868 (5)	Mean Sr1*b*—O	2.77 (8)
K1—O7^{ii}	3.048 (5)		
K1—O8	2.755 (11)	K2—O1^{iii}	2.6783 (13)
Mean K1—O	2.84 (12)	K2—O2^{ii}	2.9678 (14)
		K2—O3^{ii}	3.0315 (14)
K2—O1^{iii}	2.721 (15)	K2—O4^{iv}	3.1134 (13)
K2—O2^{ii}	2.939 (15)	K2—O11	2.7537 (12)
K2—O3^{ii}	2.973 (14)	K2—O12^{ii}	3.0513 (14)
K2—O4^{iv}	3.178 (14)	K2—O5^{v}	2.7944 (13)
K2—O11	2.771 (15)	K2—O7^{ii}	2.8994 (14)
K2—O12^{ii}	2.997 (15)	K2—O8^{ii}	3.036 (13)
K2—O5^{v}	2.823 (15)	Mean K2—O	2.90 (14)
K2—O7^{ii}	2.918 (15)		
K2—O8^{ii}	2.99 (2)	Sr2*a*—O1^{iii}	2.581 (7)
Mean K2—O	2.89 (11)	Sr2*a*—O4^{iv}	2.875 (8)
		Sr2*a*—O11	2.662 (7)
Ba2—O1^{iii}	2.67 (3)	Sr2*a*—O5^{v}	2.852 (7)
Ba2—O2^{ii}	3.02 (2)	Sr2*a*—O7^{ii}	2.857 (7)
Ba2—O3^{ii}	3.10 (2)	Mean Sr2*a*—O	2.77 (13)
Ba2—O4^{iv}	3.07 (2)		
Ba2—O11	2.75 (3)	Sr2*b*—O1^{iii}	2.619 (11)
Ba2—O12^{ii}	3.10 (3)	Sr2*b*—O2^{iii}	3.105 (11)
Ba2—O5^{v}	2.79 (3)	Sr2*b*—O4^{iv}	2.703 (8)
Ba2—O7^{ii}	2.94 (3)	Sr2*b*—O11	2.634 (11)
Ba2—O8^{ii}	3.11 (3)	Sr2*b*—O12^{i}	3.112 (10)
Mean Ba2—O	2.95 (17)	Sr2*b*—O6	2.992 (11)
		Sr2*b*—O7^{ii}	2.709 (10)
		Sr2*b*—O8	3.132 (19)
		Mean Sr2*b*—O	2.73 (15)

Symmetry codes: (i) $x, y-1, z$; (ii) $\frac{1}{2}-x, y-\frac{1}{2}, z-\frac{1}{2}$; (iii) $x-\frac{1}{2}, \frac{1}{2}-y, z$; (iv) $x-\frac{1}{2}, \frac{3}{2}-y, z$; (v) $-x, 1-y, z-\frac{1}{2}$; (vi) $\frac{1}{2}+x, \frac{1}{2}-y, z$; (vii) $1-x, 1-y, \frac{1}{2}+z$; (viii) $\frac{1}{2}-x, y-\frac{1}{2}, \frac{1}{2}+z$. Reference: (*a*) Thomas *et al.* (1990).

and is coordinated by five O atoms with one short Cr2—O bond, with a distance of 1.656 (5) Å. This suggests an oxidation state of III for Cr1 and of VI for Cr2. Typical bond lengths in pure chromium oxides are 1.96–2.01 Å for six-coordinated Cr^{III} (Sawada, 1994), 1.89–1.91 Å for six-coordinated Cr^{VI}

Table 6
Bond lengths (Å) for the Cr—O bond distances in the respective TiO_6 octahedra of SrCrKTP.

Cr1—O1	1.786 (7)	Cr2—O3	1.992 (4)
Cr1—O2^{i}	2.052 (7)	Cr2—O4^{iv}	2.055 (4)
Cr1—O11	1.869 (7)	Cr2—O12	1.656 (5)
Cr1—O12^{ii}	2.083 (7)	Cr2—O7^{iii}	1.919 (5)
Cr1—O5^{ii}	2.036 (5)	Cr2—O8	2.053 (15)
Cr1—O6^{iii}	1.980 (5)		

Symmetry codes: (i) $1-x, 1-y, z-\frac{1}{2}$; (ii) $\frac{1}{2}-x, y-\frac{1}{2}, z-\frac{1}{2}$; (iii) $\frac{1}{2}-x, \frac{1}{2}+y, z-\frac{1}{2}$; (iv) $x-\frac{1}{2}, \frac{3}{2}-y, z$.

(Burdett *et al.*, 1988) and 1.57–1.75 Å for four-coordinated Cr^{VI}, with two short and two long bonds (Stephens & Cruickshank, 1970).

EPR measurements of chromium-doped KTP (Ahn & Choh, 1999) with a dopant level entirely due to the impurity of the starting materials has shown the existence of Cr^{III} in both TiO_6 octahedra. The amount of chromium doping in SrCrKTP is magnitudes larger so somewhat different positions may be expected for the Cr^{III} atoms in the later compound, but the O—Cr—O angles measured by Ahn & Choh (1999) correlate well to those for Cr1 in SrCrKTP. The small amounts of chromium detected by EPR may behave differently in the $Ti2O_6$ octahedron than Cr2 at the present level of doping in SrCrKTP. Ahn & Choh (1999) also suggested a charge compensation model where Cr^{VI} should be located in the PO_4 tetrahedra, although there is a large difference between the P^{V} (0.35 Å) and Cr^{VI} (0.52 Å) ionic radii. In the SrCrKTP structure there is a charge compensation, but the actual position of Cr^{VI} is in the $Ti2O_6$ octahedron, removed from its centroid towards the formation of a tetrahedral coordination geometry.

There are two general ways to decrease conductivity during the growth of KTP. The first is to decrease the number of entropy-related vacancies in KTP by using a lower growth temperature while applying a high pressure. The second method is to dope KTP with trivalent cations, such as chromium, scandium or rare earth metal ions for example. Hörlin & Bolt (1995) reported that the ionic conductivity is greatly decreased in scandium- or chromium-doped KTP. The trivalent cations were supposed to be positioned inside the TiO_6 octahedra as we have shown for the SrCrKTP structure. Since the vacancies are probably due to the deficiency of oxygen in the framework, the exchange of titanium for any atom with a lower oxidation number will reduce the number of potassium vacancies. Unfortunately, both barium and strontium incorporation in KTP greatly increase the number of vacancies. Our relatively few so-called KTP double-cation exchange experiments, where the titanium and potassium sites are exchanged simultaneously, show so far that the resulting structure has a high dependence on the ratios between the additional flux substances. The SrCrKTP structural result demonstrates that it is possible to introduce two new components in KTP without any major structural changes of the framework.

Authors are grateful to Dr N. Ishizawa for assistance during the data collection. This work was supported by the Chalmers Foundation and the Australian Research Council. Financial support from the Australian Synchrotron Research Program funded by the Commonwealth of Australia *via* the Major National Research Facilities is also acknowledged. SN would like to thank the Crystallography Centre, UWA, for hospitality during the final stages of this work.

References

Ahn, S. W. & Choh, S. H. (1999). *J. Phys. Condens. Matter*, **11**, 3193–3199.
Alcock, N. W. (1974). *Acta Cryst.* A**30**, 332–335.
Almgren, J., Streltsov, V. A., Sobolev, A. N., Figgis, B. N. & Albertsson, J. (1999). *Acta Cryst.* B**55**, 712–720.
Belokoneva, E. L., Yakubovich, O. V., Tsirelson, V. G. & Urusov, V. S. (1990). *Izv. Akad. Nauk SSSR Neorg. Mater.* **26**, 595–601.
Bolt, R. J. & Bennema, P. (1990). *J. Cryst. Growth*, **102**, 329–340.
Burdett, J. K., Miller, G. J., Richardson, J. W. & Smith, J. V. (1988). *J. Am. Chem. Soc.* **110**, 8064–8071.
Burnett, M. N. & Johnson, C. K. (1996). *ORTEP*III. Report ORNL-6895. Oak Ridge National Laboratory, Tennessee, USA.
Chu, D. K. T., Hsiung, H., Cheng, L. K. & Bierlein J. D. (1993). *IEEE Trans. Ultrasonic*, **40**, 819–824.
Crennell, S. J., Cheetham, A. K., Kaduk, J. A. & Jarman, R. H. (1991). *J. Mater. Chem.* **1**, 297–298.
Crennell, S. J., Morris, R. E., Cheetham, A. K. & Jarman, R. H. (1992). *Chem. Mater.* **4**, 82–88.
Daneshvar, K., Giess, E. A., Bacon, A. M., Dawes, D. G., Gea, L. A. & Boatner, L. A. (1997). *Appl. Phys. Lett.* **71**, 756–758.
Delarue, P., Lecomte, C., Jannin, M., Marnier, G. & Menaert, B. (1999). *J. Phys. Condens. Matter*, **11**, 4123–4134.
Flack, H. D. (1983). *Acta Cryst.* A**39**, 876–881.
Furusawa, S., Hayashi, H., Ishibashi, A., Miyamoto, A. & Sasaki, T. (1993). *J. Phys. Soc. Jpn*, **62**, 183–195.
Hall, S. R., du Boulay, D. J. & Olthof-Hazekamp, R. (1999). Editors. *Xtal*3.6 *System*. University of Western Australia.
Hamilton, W. C. (1964). *Statistics in Physical Science*. New York: Ronald Press.
Hörlin, T. & Bolt, R. (1995). *Solid State Ion.* **78**, 55–62.
Karlsson, H. & Laurell, F. (1997). *Appl. Phys. Lett.* **71**, 3474–3476.
Kishimoto, S., Ishizawa, N. & Vaalsta, T. P. (1998). *Rev. Sci. Instrum.* **69**, 384–391.
Larson, A. C. (1970). *Crystallographic Computing*, edited by F. R. Ahmed, S. R. Hall and C. P. Huber, pp. 291–294. Copenhagen: Munksgaard.
Masse, R., Durif, A., Guitel, J. C. & Tordjman, I. (1972). *Bulg. Soc. Fr. Mineral. Cristallogr.* **95**, 47–55.
Nordborg, J. (2000). *Acta Cryst.* C**56**, 518–520.
Risk, W. P. & Lau, S. D. (1996). *Appl. Phys. Lett.* **69**, 3999–4001.
Roelofs, M. G., Morris, P. A. & Bierlein, J. D. (1991). *J. Appl. Phys.* **70**, 720–728.
Sasaki, S. (1989). *Numerical Tables of Anomalous Scattering factors, Calculated by the Cromer and Mann's Method.* KEK Report, 88-14, 1–136.
Sasaki, S. (1990). *X-ray Absorption Coefficients for the Elements (Li to Bi, U).* KEK Report, 90-16, 1–143.
Satow, Y. & Iitaka, Y. (1989). *Rev. Sci. Instrum.* **60**, 2390–2393.
Sawada, H. (1994). *Mater. Res. Bull.* **29**, 239–245.
Stefanovich, S., Mosunov, A., Mill, B. & Belokoneva, E. (1996). *Ferroelectrics*, **185**, 63–66.
Stephens, J. S. & Cruickshank, D. W. J. (1970). *Acta Cryst.* B**26**, 222–226.
Streltsov, V. A., Ishizawa, N. & Kishimoto, S. (1998). *J. Synchrotron Rad.* **5**, 1309–1316.
Streltsov, V. A., Nordborg, J. & Albertsson, J. (2000). *Acta Cryst.* B**56**, 785–792.

Stucky, G. D., Phillips, M. L. F. & Gier, T. E. (1989). *Chem. Mater.* **1**, 492–509.
Suma, S., Santha, N. & Sebastian, M. T. (1998). *Mater. Electr.* **9**, 39–42.
Thomas, P. A., Duhlev, R. & Teat, S. J. (1994). *Acta Cryst.* B**50**, 538–543.
Thomas, P. A., Glazer, A. M. & Watts, B. E. (1990). *Acta Cryst.* B**46**, 333–343.
Thomas, P. A. & Womersley, M. N. (1998). *Acta Cryst.* B**54**, 645–651.
Tordjman, I., Masse, R. & Guitel, J. C. (1974). *Z. Kristallogr.* **139**, 103–115.
Womersley, M. N., Thomas, P. A. & Corker, D. L. (1998). *Acta Cryst.* B**54**, 635–644.
Zachariasen, W. H. (1967). *Acta Cryst.* **23**, 558–564.